On the free-volume model of multi-shape memory effect in amorphous polymer

Xiaodong Wang[1], Yuheng Liu[1], Haibao Lu[1,3] and Yong-Qing Fu[2]

[1]Science and Technology on Advanced Composites in Special Environments Laboratory, Harbin Institute of Technology, Harbin 150080, China

[2]Faculty of Engineering and Environment, University of Northumbria, Newcastle upon Tyne, NE1 8ST, UK

[3]luhb@hit.edu.cn

Abstract: Free volume theory, which is a popular approach to solve the problems associated with glass transition in polymers, is applied to investigate multi-shape memory effect (multi-SME) of amorphous shape memory polymers (SMPs) as well. To understand the phenomena of multiple shape recovery behaviors, theories about the SME and multi-SME in amorphous SMPs are firstly developed. The thermodynamics in the SMPs with dual- and triple-SME is then investigated in the frameworks of the free volume model and Eyring equation, taking account of the dependencies of free volume and activation energy on relaxation time. Finally, the proposed free volume model is evaluated and compared with results from the amorphous SMPs with dual- and triple-SMEs. Results from our newly proposed model show a good agreement with experimental results obtained at different temperatures.

Keywords: free volume model, shape memory polymer, multi-shape memory effect

1. Introduction

Shape memory polymers (SMPs) are one kind of stimulus-responsive materials which, after a programmed process, has their unique ability to fix one temporary shape and regain their original shape upon to a suitably external stimulus, such as heat, light, electricity, solvent, or magnetic field [1-5]. Conventional SMPs have specified shape transition temperatures and present dual-shape memory effect (dual-SME), and they have been developed to a wide range of applications from biomedicine [6-8] to civil engineering [9-11] in the last four decades.

Recently, there has been a great interest in the development of SMPs with multi-SME [12-15], which is originated from the multiple reversible transition phases with well-separated glass transition temperature zone and then segmental relaxations [14,16,17]. In molecular scales, there are many segments of different properties tangled together in macromolecule chains [18], and the reversibly configurational entropy generating from the multi-stage glass transitions enables generation of multi-SME associated with the macromolecule chains [19]. Therefore, multi-stage glass transitions and reversibly configurational entropy have been identified as the main driving force for multi-SME in amorphous SMPs [20]. In terms of thermodynamics, shape memory behavior is originated from the viscoelastic relaxation of segments within the SMPs [21-25]. Therefore, temperature and time are two key factors that need to be taken into account for the constitutive modelling of SMPs with multi-SME [21-27]. In previous studies, the time-dependent constitutive relations of dual-SMPs were typically investigated using multi-branch Maxwell

models [21-25]. Results showed that the relaxation time vs. temperature is based on the Eyring equation [26] when the temperature is lower than the glass transition temperature (T_g); whereas it is ruled by the WLF equation [27] when the temperature is higher than T_g. These models have been found to be well suitable to characterize the constitutive relationship of time-dependent thermomechanical behaviors. However, these phenomenological studies generally need huge effort in both computations and experimental measurements because the relaxation behaviors of all segments should be considered.

Free volume is an important parameter which can be linked with the properties of polymers [27]. In a glassy state, the motion of polymer chains is restricted. Therefore, the free volume is hardly changed below the T_g [28], while the volume is only caused by the polymer substance itself [29,30]. On the other hand, all of the volume change is attributed to the free volume when the polymer is in its rubbery state [27].

In this study, we establish a new hybrid model by reconsidering the Eyring equation [31,32] integrated with free volume theory [33,34] on describing the multi-SME in SMPs undergoing multiple glass transitions. Boltzmann's superposition principle [35] is then employed to couple the overall cooperative relaxations during the transition processes. Dependences of elastic modulus and stored strain upon the temperature and relaxation time are theoretically investigated using this newly proposed model. Finally, the simulation results are compared with the experimental data reported in the literature [36,37] for further verification.

2. Modelling of SMP with dual-SME

SMP is composed of hard segments and soft ones in the molecule chains [36]. The hard segment is functioned to remember the original shape of the SMP, while the soft one undergoes a reversible configuration relaxation to respond to the external stimuli [36]. To express this unique molecular structure, the Eyring equation was previously combined with the WLF equation to characterize the thermodynamics of SMP [31]. For the polymer, it needs sufficient activation energy to overcome the energy barrier in its glassy state, while it needs free volume available to jump in its rubbery state [38]. Therefore, the probability of a polymer molecule to relax (p_j) around the T_g can be simply written as:

$$p_j = p_e \cdot p_v \tag{1}$$

where p_e is the probability of SMP to obtain sufficient activation energy to overcome the energy barrier, and p_v is the probability of SMP to obtain enough free volume available to jump.

To calculate the value of p_v, it is assumed that each molecule is confined within a space made up of its neighbors. According to the hard-sphere free volume theory [33], $P(v)$ is the probability of relaxation determined by the free volume (v) and writes:

$$P(v) = (\gamma / v_f) \exp(-\gamma v / v_f) \tag{2}$$

where v_f is the average free volume per molecule, and γ is a given constant which is used to correct the overlap of free volume ($0.5 \le \gamma \le 1$) [33]. Assuming that the minimum value of free volume is v_0, equation (2) can therefore be written as:

$$p_v = \int_{v_0}^{\infty} P(v)dv = \int_{v_0}^{\infty} (\gamma / v_f) \exp(-\gamma v / v_f)dv = \exp(\frac{-\gamma v_0}{v_f}) = \exp(\frac{-\gamma V_0}{V_f}) \tag{3}$$

where V_0 is the volume of the occupied molecules and V_f is the free volume in polymer. V_0 and V_f can be expressed as:

$$V_0 = v_0 \cdot N \quad V_f = v_f \cdot N \tag{4}$$

where N is the number of molecules.

Based on the Doolittle equation [31,34], the free volume (V_f) is fully resulted from thermal expansion at the constant pressure:

$$V_f = V - V_0 - V^{'} = V_0 \left\{ \exp\left[\int_0^T \alpha(T) dT \right] - 1 \right\} \tag{5}$$

where $\alpha(T)$ is the coefficient of thermal expansion, V is the total volume of the polymer, and $V^{'}$ is the volume of hard segment. If $(V - V^{'})\alpha$ is kept a constant [31], equation (5) can be rewritten as:

$$V_f = \alpha(V - V^{'})(T - T_0) \tag{6}$$

where T_0 is the initial temperature where the relaxation of soft segment is confined in one space unit and V_f =0 according to the Adam-Gibbs model [39].

By substituting equation (6) into equation (3), we can get:

$$p_v = \exp(\frac{-\gamma V_0}{V_f}) = \exp(\frac{-\gamma V_0}{\alpha(V - V^{'})(T - T_0)}) \tag{7}$$

Because the parameter of γ, V_0 and $\alpha(V - V^{'})$ are all constants, we introduce a parameter $\omega = \gamma V_0 / [\alpha(V - V^{'})]$ into equation (7). Therefore, it can be written as:

$$p_v = \exp(-\omega / (T - T_0)) \tag{8}$$

Furthermore, p_e is the probability of the SMP to obtain sufficient activation energy, which is ruled by the Eyring equation [40]:

$$p_e = A_0 T^m \exp(-\frac{E_a}{RT}) \tag{9}$$

where $R=8.314\ J/(mol\cdot K)$ is the gas constant, A_0 is the pre-exponential coefficient, m is a given constant and E_a is the activation energy. Based on the previous study [41], the temperature-dependent activation energy can be expressed as,

$$E_a = E_{a0} - \left(\frac{T_h - T}{b\cdot T_h - T}\right)RT \tag{10}$$

where E_{a0} is the initial activation energy, T_h is the complete transition temperature and b is a material constant.

By substituting equation (10) into equation (9), we can obtain:

$$p_e = A_0 T^m \exp\left[-\frac{E_{a0}}{RT} + \left(\frac{T_h - T}{b\cdot T_h - T}\right)\right] \tag{11}$$

In combination of equation (1), equation (8) and equation (11), we can obtain the probability of the molecules in their frozen phase p_j:

$$p_j = p_e \cdot p_v = A_0 T^m \exp\left\{-\omega/(T - T_0) - \frac{E_{a0}}{RT} + \left(\frac{T_h - T}{b\cdot T_h - T}\right)\right\} \tag{12}$$

Here an empirical relationship between T_g and T_0 is introduced as [38]:

$$T_0 = T_g / \exp((T_g / C_2^{'}) - 1)^{-1} \tag{13}$$

where $C_2^{'}$ is a given constant according to WLF equation [27]. In combination of equation (12) and equation (13), the probability p_j can be finally obtained:

$$p_j = p_e \cdot p_v = A_0 T^m \exp\left\{-\omega/(T - T_g/\exp((T_g/C_2^{'}) - 1)^{-1}) - \frac{E_{a0}}{RT} + \left(\frac{T_h - T}{b\cdot T_h - T}\right)\right\} \tag{14}$$

Based on the phase transition theory [36], the phase evolution function (ϕ_f) is used for the volume fraction of the frozen phase in the soft segment. If the thermal expansion strain is negligible, the phase evolution function is then determined by the stored strain (ε^*) and pre-stored strain (ε_{pre}). Therefore, the phase evolution function

can be further expressed as follows [36]:

$$\phi_f = \frac{\varepsilon^*}{\varepsilon_{pre}} = 1 - p_j = 1 - A_0 T^m \exp\left\{-\omega / (T - T_g / \exp((T_g / C_2^{'}) - 1)^{-1}) - \frac{E_{a0}}{RT} + \left(\frac{T_h - T}{b \cdot T_h - T}\right)\right\} \quad (15)$$

According to equation (15), the volume fraction of the active phase in the soft segment (ϕ_a) can be obtained:

$$\phi_a = 1 - \phi_f = A_0 T^m \exp\left\{-\omega / (T - T_g / \exp((T_g / C_2^{'}) - 1)^{-1}) - \frac{E_{a0}}{RT} + \left(\frac{T_h - T}{b \cdot T_h - T}\right)\right\} \quad (16)$$

According to the Mori-Tanaka equation [42], the effective storage modulus of the soft segment (E_s) can be written as the functions of ϕ_a and ϕ_f:

$$E_s(T) = K_f \left(1 + \frac{\phi_a (K_a / K_f - 1)}{1 + \xi \phi_f (K_a / K_f - 1)}\right) \quad (17)$$

where ξ is a given constant, K_a and K_f are the moduli of active phase and frozen phase of soft segment, respectively.

The temperature dependence of the modulus ($E_h(T)$) of hard segment in the glassy state can be written as [43]:

$$\log E_h(T) = \log E(T^{ref}) - a(T - T^{ref}) \quad (18)$$

where $E(T^{ref})$ is the Young's modulus at the referenced temperature (T^{ref}) and a is a material constant.

Here, the contribution of the hard and soft segments to the bulk modulus ($E(T)$) of the SMP is assumed in a parallel manner. Based on the Takayanagi principle [24,44], the bulk modulus $E(T)$ can be therefore obtained as:

$$\frac{1}{E} = \frac{\beta}{E_s} + \frac{1 - \beta}{E_h} = \beta / \left[K_f \left(1 + \frac{\phi_a (K_a / K_f - 1)}{1 + \xi \phi_f (K_a / K_f - 1)}\right)\right] + \frac{1 - \beta}{\exp\left[\log E(T^{ref}) - a(T - T^{ref})\right]} \quad (19)$$

where β ($0 < \beta < 1$) is the volume fraction of soft segment.

Shape recovery stress (σ_{relx}) is another important parameter to determine the shape memory behavior of SMPs [45,46]. It is resulted from the relaxations of soft segments and can be expressed as [35,47]:

$$\sigma_{relx} = \sum_{i=1}^{n} \sigma_i \exp(-t/\tau_i) \tag{20}$$

where σ_i and τ_i are the recovery stress and relaxation time of the *i*th soft segment, respectively, *n* is the number of soft segments and *t* is the relaxation time of SMP. Therefore, the recovery stress of the SMP with one hard segment and one soft one can be written as,

$$\sigma_{relx} = \phi_f \sigma_f \exp(-t/\tau_f) + \phi_a \sigma_a \tag{21}$$

where σ_f is the recovery stress of the soft segment in the glassy state, σ_a is the recovery stress in the rubbery state and τ_f is the relaxation time of soft segment in the glassy state.

In the glassy state, the relaxation time τ_f with respect to temperature follows the Eyring form [26] and can be written as:

$$\tau_f = \tau_{f0} \alpha_T(T) = \tau_{f0} \exp\left[-\theta\left(\frac{1}{T} - \frac{1}{T_g}\right)\right] \tag{22}$$

where τ_{f0} is the referenced relaxation time and parameter θ is the given material constant.

When the SMP is heated at a constant heating rate ($\dot{T}$), the relaxation time t of SMP can be determined from:

$$t = (T - T')/\dot{T} \tag{23}$$

where T' is the initial temperature.

By substituting equation (22) and equation (23) into equation (21), the recovery stress (σ_{relx}) can be obtained as:

$$\sigma_{relx}=\phi_f\sigma_f\exp\left\{-(T-T')/\left\{T\tau_{f0}\exp\left[-\theta(\frac{1}{T}-\frac{1}{T_g})\right]\right\}\right\}+\phi_a\sigma_a \tag{24}$$

3. Theoretical framework

To further investigate the SMP with multi-SME, the temperature and time dependent probability of a molecule to overcome the energy barrier (p_e) to relax is introduced as [48]:

$$p_e(T,t)=1-[1-\exp(-\Delta H(T)/RT)]^{vt} \tag{25}$$

where $\Delta H(T)$ is the activation energy per mole, v is the correction factor and t is the relaxation time. The activation energy ($\Delta H(T)$) can be written as [49]:

$$\Delta H(T)=\kappa R/(1-T_r/T)^2 \tag{26}$$

where κ and T_r are the given constants.

In combination of equation (25) and equation (26), equation (25) can be rewritten as:

$$p_e(T,t)=1-\left\{1-\exp(-\kappa/\left[(1-T_r/T)^2T\right])\right\}^{vt} \tag{27}$$

By substituting equation (8) and equation (27) into equation (1), we can obtain the probability of the transition for the molecules (p_j) as:

$$p_j(T,t)=\left\{1-\left\{1-\exp(-\kappa/\left[(1-T_r/T)^2T\right])\right\}^{vt}\right\}\exp\left[-\omega/(T-T_0)\right] \tag{28}$$

Therefore, equation (15) can also be written as:

$$\begin{aligned}\phi_f(T,t)&=\frac{\varepsilon^*}{\varepsilon_{pre}}=1-p_j\\&=1-\left\{1-\left\{1-\exp(-\kappa/\left[(1-T_r/T)^2T\right])\right\}^{vt}\right\}\exp\left\{-\omega/\left[T-T_g/\exp\left(\frac{T_g}{C_2'}-1\right)^{-1}\right]\right\}\end{aligned} \tag{29}$$

According to the Boltzmann's superposition principle [35], the multi-SME is

originated from relaxations of all the segments in the SMP, therefore, it is:

$$\varepsilon^* = \sum_{i=1}^{n} \phi_{f_i}(T,t)\varepsilon_{pre}(i) \tag{30}$$

where $\phi_{f_i}(T,t)$ and $\varepsilon_{pre}(i)$ are the phase evolution function and the pre-loading strain of the ith soft segment, respectively.

For the SMPs with the multi-SMEs, the polymers are incorporated with one hard segment and multiple soft segments. Therefore, the storage modulus of the SMP is determined by those of all its segments. In combination of equation (19) and equation (30), the storage modulus of the SMP can be obtained as:

$$\frac{1}{E} = \sum_{i=1}^{n}\left(\beta_i / E_s(i)\right) + (1 - \sum_{i=1}^{n}\beta_i) / E_h \tag{31}$$

where β_i and $E_s(i)$ is the volume fraction and the modulus of the ith soft segment, and E_h is the modulus of the hard segment.

Here, the dual- and multi-SME in SMPs are modeled by the free volume theory and Eyring equation. There are a large number of material parameters in the proposed models. To easily understand the physical meaning of these parameters, they all have been listed in Table 1.

[Table 1]

4. Modelling and experimental verification of SMP with multi-SME

Initially, to investigate the effect of the glass transition temperature on the phase evolution function (ϕ_f), the simulation results obtained using equation (15) are plotted in Figure 1(a), which are also compared with experiment data reported in Ref. [36]. The used parameter values in equation (15) are presented in Table 2. The

Universal Global Algorithm (UGO) method is adopted to determine the values of parameters in the proposed models. The convergence tolerance is set as 1×10^{-10} and the maximum iteration is set as 1000. Equation (15) is used to compare with the experimental data of free recovery behavior to determine the values of parameters, e.g. A_0, m, ω, $C_2^{'}$, E_{a0}, T_h and b. And then, equation (19) is used to compare with dynamic mechanical analysis (DMA) results to determine the values of parameters, e.g. β, ξ, K_a, K_f, $E(T^{ref})$, a and T^{ref}.

It can be seen that the phase evolution function (ϕ_f) is gradually decreased with an increase in temperature, which indicate that more volume fraction of soft segment has been transformed from frozen phase to active one. To further investigate the effect of T_g on the phase evolution function (ϕ_f), the numerical results of phase evolution function (ϕ_f) as a function of temperature have been obtained and plotted in Figure 1(b). Simulation results clearly reveal that the transformation of phase evolution function (ϕ_f) is completed at the temperature increased from 332.6 *K* to 349.5 *K* with T_g of SMP increased from 330 *K* to 345 *K*.

[Table 2]

[Figure 1]

The theoretical results of storage modulus (obtained using equation (19)) as a function of temperature are presented in Figure 2, and the values of parameters used in equation (19) are listed in Table 3. The numerical results reveal that the storage modulus of the SMP is 772.8 *MPa* when the phase evolution function ϕ_f=1 at 310 *K*. Then it is gradually decreased to 36.81 *MPa* when the SMP is heated to 343 *K*. These

simulation results calculated based on equation (19) fit well with the experimental data.

[Table 3]

[Figure 2]

Effect of phase evolution function (ϕ_f) on the stored strain is further investigated according to the equation (15). As shown in Figure 3, the obtained results of stored strain fit well with the experimental data obtained from the tensile and compressive tests [36]. The temperature dependent stored strain of SMP is also determined by the phase evolution function (ϕ_f) of soft segment. With the phase evolution function (ϕ_f) decreased from 1 to 0, the stored strain in the SMP is found to gradually decreased from ±9.1% to 0%.

[Figure 3]

The theoretical results of recovery stress using equation (24) were obtained and compared with experimental data [36]. The values of parameters used in equation (24) are listed in Table 4. As revealed in Figure 4, the recovery stress is as high as 1.32 *MPa* where the soft segment is in the glassy state, and the phase evolution function is kept as ϕ_f=1 at a temperature of 310 *K*. With an increase in the temperature, the recovery stress is gradually decreased owing to the decrease in the phase evolution function from ϕ_f=1 to ϕ_f=0. It is finally decreased to 0.74 *MPa* when the SMP is heated to the T_g (T_g=343 *K*). To reveal the dynamics of recovery stress depending on temperature, the derivative stress curve is also plotted. It is revealed that the derivative stress achieves to its maximum value in the temperature range of 343 *K* to

355 *K*, which is in the glass transition temperature range.

[Table 4]

[Figure 4]

The stored strain as a function of time has been plotted in Figure 5, while the numerical results using equation (30) and experimental data [37] have also been presented for comparisons. The values of parameters used in equation (15) and equation (30) are listed in Table 5.

As shown in Figure 5(a), the SMP was heated from 297 K to 329 K at a heating rate of 1.8 K/min. Then it was kept at 329 K for 8 min. Finally the SMP was heated again from 329 K to 357 K at a heating rate of 2.0 K/min. Both simulation and experimental results reveal that the stored strain is gradually released and decreased with an increase in the temperature from 297 K to 329 K. Then it is gradually decreased when the temperature is kept at 329 K. Furthermore, the stored strain of SMP continues to decrease with a further increase in the temperature from 329 K to 357 K.

As discussed in a previous study [37], the SMP undergoes two-stage glass transition resulted from the existence of two soft segments. Therefore, the stored strains of two soft segments have been plotted in Figure 5(b). It is revealed that the stored strain of the first soft segment is gradually decreased from 0.024 to 0.007 in the temperature range from 297 K to 357 K, while the stored strain of the second one is gradually decreased from 0.023 to 0 in the temperature range from 339 K to 357 K. These simulation results reveal that the stored strain of SMP is determined by the superposition of the relaxation of both soft segments.

[Table 5]

[Figure 5]

After the thermomechanical modulus, recovery strain and stress have been discussed, now we will explore the working mechanism of probability of activation energy (p_e) and probability of free volume (p_v) in the SMP with a triple-SME. Figure 6 shows the stored strain as a function of time at a constant heating rate. At 310 K, the stored strain in the first soft segment of the SMP is completely released and it is then kept a constant in the temperature range of 310 K to 335 K. Consequently, the stored strain of SMP is gradually released when the temperature is above 335 K. However, the stored strain reaches to 0.005 at 357 K, while the stored strain is 0 when it is only determined by the activation energy. Therefore, these simulation results reveal that there is no cooperative interaction between the first and second soft segments if the relaxation behavior is only determined by the activation energy. However, we should point out that the cooperative interaction is actually resulted from the free volume.

[Figure 6]

To further quantitatively investigate the effect of temperature on the probability of activation energy (p_e) and probability of free volume (p_v) of the SMP, we have obtained the simulation results of the function of p_e / p_v with respect to temperature as shown in Figure 7. In the first transition process of the soft segment, it is found that the effect of probability of activation energy (p_e) on the SMP is gradually increased in the temperature range from 297 K to 306 K, while the probability of free volume

(p_v) plays an more important role in influencing the thermomechanical properties of the SMP in the temperature range of 306 K to 357 K. On the other hand, the activation energy will influence the second transition process after 335 K. These simulation results reveal that the phase transition of the triple-SMPs is resulted from the Boltzmann's superposition principle of the relaxation behavior of two soft segments.

[Figure 7]

Here equation (31) is utilized to characterize the storage moduli of the SMP with triple-SME and then to compare with the experimental data [37] for verification. The comparisons have been presented in Figure 8, while the corresponding parameters used in equation (31) are listed in Table 4. For the parameters of hard segment, they are T^{ref} =240K, $E(T^{ref})$ =3000MPa and a =0.32 [37]. It is found that the simulation results show better agreements with the experimental ones. The calculated results of the proposed model present a two-stage transition in the temperature ranges of (1) 300ºC to 322ºC; and (2) 335ºC to 360ºC, respectively, during which the storage moduli present a two-state transition of (1) 1995.2 MPa to 75 MPa; and (2) 75MPa to 8.3 MPa. The numerical analysis results prove that the proposed model is suitable to describe the thermomechanical properties and fit well with the experimental data of the SMP with a triple-SME.

[Figure 8]

To expand the free-volume model for the multi-SME, it is assumed that a SMP has four different soft segments, whose T_g s are 330 K, 360 K, 390 K and 420 K. The pre-strain (ε_{pre}) and volume fraction (ϕ_f) are ε_{pre} =0.25 and ϕ_f =0.25, respectively.

The numerical results of the stored strains of SMP with four soft segments are plotted in Figure 9. These simulation results present that the stored strain of SMP is significantly determined by those of the segments. Furthermore, it is applicable to achieve and design the multi-SME by means of changing the T_g and volume fraction (ϕ_f) of the segment components, according to our newly proposed free volume model.

[Figure 9]

5. Conclusion

In this study, a newly proposed hybrid model was used to describe the unique characteristics of the segmental relaxations and dynamic phase transitions of the SMP with dual-, triple- and multi-SMEs. Effects of both activation energy and free volume on the stored strains and storage moduli were systematically studied. It is found that the free volume is the driving force for the cooperative interactions among the relaxations of segments, and it plays a similar role as the activation energy to determine the relaxation behavior when the segments are in their rubbery states. The combination of the Mori-Tanaka equation and Takayanagi principle is firstly used to characterize the constitutive relationship of thermomechanical behavior of the SMP. Furthermore, the experimental results have been employed to validate the simulation results of the proposed model for the SMP with dual- and triple-SME, and a good agreement has been found. Finally, the working mechanism of probability of free volume (p_v) has been identified and it is expected to provide a theoretical guidance for the design of multi-SME in SMPs.

Acknowledgements

This work was financially supported by the National Natural Science Foundation of China (NSFC) under Grant No. 11672342 and 11725208, Newton Mobility Grant (IE161019) through Royal Society and NFSC.

Reference

[1] Wu Y, Hu J, Zhang C, Han J, Wang Y and Kumar B 2015 A facile approach to fabricate a UV/heat dual-responsive triple shape memory polymer *J. Mater. Chem. A* **3** 97-100

[2] Lu H, Yao Y, Huang W M and Hui D 2014 Noncovalently functionalized carbon fiber by grafted self-assembled graphene oxide and the synergistic effect on polymeric shape memory nanocomposites *Compos. Part B Eng.* **67** 290-5

[3] Lendlein A, Jiang H, Junger O and Langer R 2005 Light-induced shape-memory polymers *Nature* **434** 879-82

[4] Mohr R, Kratz K, Weigel T, Lucka-Gabor M, Moneke M and Lendlein A 2006 Initiation of shape-memory effect by inductive heating of magnetic nanoparticles in thermoplastic polymers *Proc. Natl. Acad. Sci.* **103** 3540-5

[5] Huo Y, Bi X, Liu Z, You Z, Lv Z, He C, Sun L, Fan X, Guo Y and Chen S 2018 A biodegradable functional water-responsive shape memory polymer for biomedical applications *J. Mater. Chem. B* **7** 123-32

[6] Wischke C, Neffe A T, Steuer S and Lendlein A 2009 Evaluation of a degradable shape-memory polymer network as matrix for controlled drug release *J. Control. Release* **138** 243-50

[7] Yu Y and Ikeda T 2005 Photodeformable polymers: A new kind of promising smart material for micro- and nano-applications *Macromol. Chem. Phys.* **206** 1705-8

[8] Nagahama K, Ueda Y, Ouchi T and Ohya Y 2009 Biodegradable shape-memory polymers exhibiting sharp thermal transitions and controlled drug release *Biomacromolecules* **10** 1789-94

[9] Meiorin C, Aranguren M I and Mosiewicki M A 2012 Vegetable oil/styrene thermoset copolymers with shape memory behavior and damping capacity *Polym. Int.* **61** 735-42

[10] Maitland D J, Small W, Ortega J M, Buckley P R, Rodriguez J, Hartman J and Wilson T S 2007 Prototype laser-activated shape memory polymer foam device

for embolic treatment of aneurysms *J. Biomed. Opt.* **12** 030504

[11] Meng H and Li G 2013 A review of stimuli-responsive shape memory polymer composites *Polymer* **54** 2199-221

[12] Nöchel U, Kumar U N, Wang K, Kratz K, Behl M and Lendlein A 2014 Triple-shape effect with adjustable switching temperatures in crosslinked poly[ethylene-co-(vinyl acetate)] *Macromol. Chem. Phys.* **215** 2446-56

[13] Ware T, Hearon K, Lonnecker A, Wooley K L, Maitland D J and Voit W 2012 Triple-shape memory polymers based on self-complementary hydrogen bonding *Macromolecules* **45** 1062-9

[14] Chatani S, Wang C, Podgórski M and Bowman C N 2014 Triple shape memory materials incorporating two distinct polymer networks formed by selective thiol-Michael addition reactions *Macromolecules* **47** 4949-54

[15] Behl M, Bellin I, Kelch S, Wagermaier W and Lendlein A 2009 One-step process for creating triple-shape capability of AB polymer networks *Adv. Funct. Mater.* **19** 102-8

[16] Ge Q, Luo X, Iversen C B, Mather P T, Dunn M L and Qi H J 2013 Mechanisms of triple-shape polymeric composites due to dual thermal transitions *Soft Matter* **9** 2212-23

[17] Yu K, Xie T, Leng J, Ding Y and Qi H J 2012 Mechanisms of multi-shape memory effects and associated energy release in shape memory polymers *Soft Matter* **8** 5687-95

[18] Xie T 2010 Tunable polymer multi-shape memory effect *Nature* **464** 267-70

[19] Lu H, Wang X, Xing Z and Fu Y-Q 2019 A cooperative domain model for multiple phase transitions and complex conformational relaxations in polymers with shape memory effect *J. Phys. D. Appl. Phys.* **52** 245301

[20] Nguyen T D, Jerry Qi H, Castro F and Long K N 2008 A thermoviscoelastic model for amorphous shape memory polymers: Incorporating structural and stress relaxation *J. Mech. Phys. Solids* **56** 2792-814

[21] Fang C, Leng J, Sun H and Gu J 2018 A multi-branch thermoviscoelastic model based on fractional derivatives for free recovery behaviors of shape memory

polymers *Mech. Mater.* **120** 34-42

[22] Ge Q, Yu K, Ding Y and Jerry Qi H 2012 Prediction of temperature-dependent free recovery behaviors of amorphous shape memory polymers *Soft Matter* **8** 11098-105

[23] Lei M, Yu K, Lu H and Qi H J 2017 Influence of structural relaxation on thermomechanical and shape memory performances of amorphous polymers In fl uence of structural relaxation on thermomechanical and shape memory performances of amorphous polymers *Polymer* **109** 216-28

[24] Lu H, Wang X, Yu K, Fu Y Q and Leng J 2019 A thermodynamic model for tunable multi-shape memory effect and cooperative relaxation in amorphous polymers *Smart Mater. Struct.* **28** 1-43

[25] Castro F, Westbrook K K, Long K N, Shandas R and Qi H J 2010 Effects of thermal rates on the thermomechanical behaviors of amorphous shape memory polymers *Mech. Time-Dependent Mater.* **14** 219-41

[26] Di Marzio E A and Yang A J M 2012 Configurational entropy approach to the kinetics of glasses *J. Res. Natl. Inst. Stand. Technol.* **102** 135

[27] Williams, M L, Landel, R F and Ferry, J D 1955 The temperature dependence of relaxation mechanisms in amorphous polymers and other glass-forming liquids. *J. Am. Chem. Soc.* **77** 3701-7

[28] Macedo P B and Litovitz T A 1965 On the relative roles of free volume and activation energy in the viscosity of liquids *J. Chem. Phys.* **42** 245-56

[29] Simiha R and Boyer R 1962 On a General Relation Involving the Glass Temperature and Coefficients of Expansion of Polymers *J. Appl. Phys.* **37** 1003

[30] Fox T G and Flory P J 1950 Second-order transition temperatures and related properties of polystyrene. I. Influence of molecular weight *J. Appl. Phys.* **21** 581-91

[31] Macedo P B and Litovitz T A 1965 On the relative roles of free volume and activation energy in the viscosity of liquids *J. Chem. Phys.* **42** 245-56

[32] Kincaid J F, Eyring H and Stearn A E 1941 The theory of absolute reaction rates and its application to viscosity and diffusion in the liquid state *Chem. Rev.* **28**

301-65

[33] Cohen M H and Turnbull D 1959 Molecular transport in liquids and glasses *J. Chem. Phys.* **31** 1164-9

[34] Doolittle A K 1951 Studies in Newtonian Flow. II. The Dependence of the Viscosity of Liquids on Free-Space *J. Appl. Phys.* **22** 1471

[35] Westbrook K K, Kao P H, Castro F, Ding Y and Jerry Qi H 2011 A 3D finite deformation constitutive model for amorphous shape memory polymers: A multi-branch modeling approach for nonequilibrium relaxation processes *Mech. Mater.* **43** 853-69

[36] Liu Y, Gall K, Dunn M L, Greenberg A R and Diani J 2006 Thermomechanics of shape memory polymers: Uniaxial experiments and constitutive modeling *Int. J. Plast.* **22** 279-313

[37] Xie T, Xiao X and Cheng Y T 2009 Revealing triple-shape memory effect by polymer bilayers *Macromol. Rapid Commun.* **30** 1823-7

[38] Gibbs J H and Adam G 1965 On the Temperature Dependence of Cooperative Relaxation Properties in Glass-Forming Liquids *J. Chem. Phys.* **43** 139-46

[39] Matsuoka S and Quan X 1991 Intermolecular cooperativity in dielectric and viscoelastic relaxation *J. Non. Cryst. Solids* **131** 293-301

[40] Adams P A, Sheppard J G, Ridler G M and Ridler P F 1978 New three-parameter empirical extension of the arrhenius equation suitable for the precise evaluation of pseudo-thermodynamic activation parameters in chemical kinetics *J. Chem. Soc. Faraday Trans. 1 Phys. Chem. Condens. Phases* **74** 1500-6

[41] Lu H, Wang X, Yu K, Huang W M, Yao Y and Leng J 2017 A phenomenological formulation for the shape/temperature memory effect in amorphous polymers with multi-stress components *Smart Mater. Struct.* **26** 095011

[42] Weng G J 1984 Some elastic properties of reinforced solids, with special reference to isotropic ones containing spherical inclusions *Int. J. Eng. Sci.* **22** 845

[43] Arruda E M and Boyce M C 1993 Evolution of plastic anisotropy in amorphous polymers during finite straining *Int. J. Plast.* **9** 697-720

[44] Wang X, Lu H, Shi X, Yu K and Fu Y Q 2019 A thermomechanical model of

multi-shape memory effect for amorphous polymer with tunable segment compositions *Compos. Part B Eng.* **160** 298-305

[45] Xue L, Dai S and Li Z 2010 Biodegradable shape-memory block co-polymers for fast self-expandable stents *Biomaterials* **31** 8132-40

[46] Venkatraman S S, Tan L P, Joso J F D, Boey Y C F and Wang X 2006 Biodegradable stents with elastic memory *Biomaterials* **27** 1573-8

[47] Yang Q and Li G 2016 Temperature and rate dependent thermomechanical modeling of shape memory polymers with physics based phase evolution law *Int. J. Plast.* **80** 168-86

[48] Zwanzig R 2001 Nonequilibrium statistical mechanics *Oxford University Press, Oxford*

[49] Bauer T, Lunkenheimer P and Loidl A 2013 Cooperativity and the freezing of molecular motion at the glass transition *Phys. Rev. Lett.* **111** 225702

Tables caption

Table 1. Summary of parameters.

Table 2. Value of parameters used in equation (15).

Table 3. Value of parameters used in equation (19).

Table 4. Value of parameters used in equation (24).

Table 5. Value of parameters used in equation (30) and equation (31).

Figures caption

Figure 1. (a) Comparison between the simulation result of Eq. (15) and the experiment data [36] of the SMP. (b) Phase evolution function as a function of temperature at T_g=330 K, 335 K, 340 K and 345 K.

Figure 2. Comparison of the simulation results of equation (19) and the experimental data [36] of the storage modulus as a function of temperature.

Figure 3. Comparison of the simulation results of equation (15) and the experimental data [36] of the tensile and compressive stored strains as a function of temperature.

Figure 4. Comparison of the simulation results of equation (24) and the experimental data [36] of the recovery stress and the derivative stress as a function of temperature.

Figure 5. (a) Comparison between simulation results of equation (30) and experimental data [37] of the stored strain as a function of time. (b) Simulation results of stored strains of two soft segments in SMP with triple-SME.

Figure 6. Numerical result of the stored strain in two soft segments of SMP at a constant heating rate. One is determined by the probability of activation energy (p_e), while the other is determined by both the probability of activation energy (p_e) and probability of free volume (p_v).

Figure 7. Numerical results of the p_e / p_v with respect to temperature of the first transition phase and the second transition phase of two soft segments, respectively.

Figure 8. Comparison between simulation results of equation (31) and the experimental data [37] of SMP with triple-SME.

Figure 9. Numerical results for the stored strain as a function of relaxation time for the SMP with quintuple-SME.

Table 1.

p_j	The probability of a polymer molecule to relax around the T_g	p_e	The probability to obtain sufficient energy to overcome the barrier
p_v	The probability of SMP to obtain enough free volume available to jump	v_f	The average free volume per molecule
γ	A given constant which is used to correct the overlap of free volume	V_0	The volume of the occupied molecules
V_f	The free volume in polymer.	V	The total volume of the polymer
N	The mol number of molecules	$\alpha(T)$	The coefficient of thermal expansion
T_0	The zero-entropy temperature	A_0	The pre-exponential coefficient
E_{a0}	The initial activation energy	T_h	The complete transition temperature
b	A constant related to the internal stress	$C_2^{'}$	A constant related to WLF equation
ϕ_f	The volume fraction of the frozen phase	ϕ_a	The volume fraction of the active phase
E_s	The effective storage modulus of the soft segment	E_h	The storage modulus of the hard segment
K_a	The moduli of active phase	K_f	The moduli of frozen phase
$E(T^{ref})$	The Young's modulus at the referenced temperature (T^{ref})	a	The material constant related to the Young's modulus
β_i	The volume fraction of the ith soft segment	σ_s	The recovery stress of the soft segment in the glassy state
σ_a	The recovery stress in the rubbery state	τ_{f0}	The referenced relaxation time
n	The number of soft segments	ξ	A given constant in the Mori-Tanaka equation

Table 2.

A_0	m	ω	$C_2^{'}$ (K)	E_{a0} (KJ/mol)	T_h (K)	b
0.082	1.0	165.85	36.02	70	358	1.018

Table 3.

β	ξ	$K_a(MPa)$	$K_f(MPa)$	$E(T^{ref})(MPa)$	a	$T^{ref}(K)$
0.6	0.98	0.35	900	1866	0.0437	285.43

Table 4.

σ_f (MPa)	σ_a (MPa)	τ_{f0} (min)	θ
4	0.75	29.23	2035.17

Table 5.

Parameter	The 1st transition phase	The 2nd transition phase
ε_{pre}	0.0240	0.0232
κ	1	12.1
T_r (K)	292.9	317.0
ν (1/min)	1.54	49.9
ω	12.3	1.2
T_g (K)	330	353
$C_2^{'}$ (K)	31.36	49.39
β	0.44	0.559
K_f (MPa)	2180.68	1828.49
K_a (MPa)	13.77	3.77
ξ	1.236	1.002

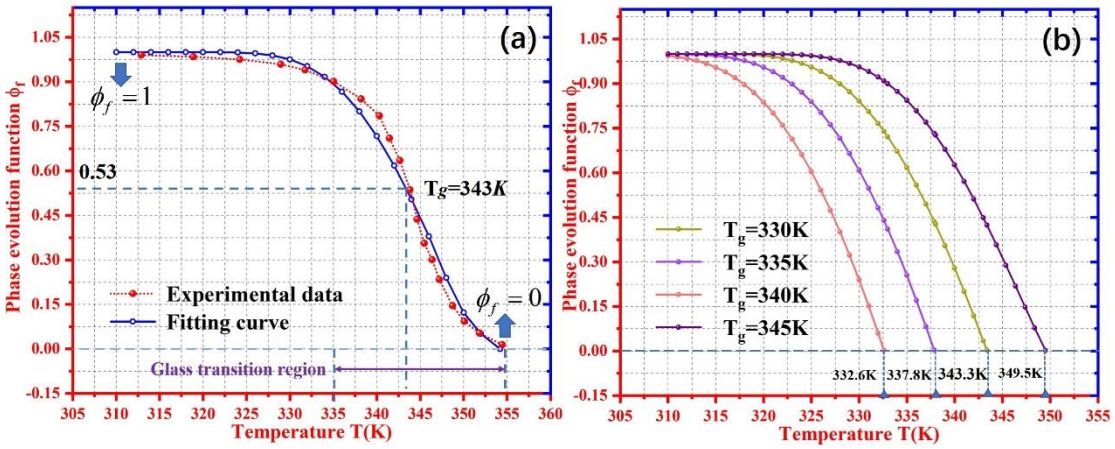
(a)
$\phi_f = 1$
0.53
Tg=343K
$\phi_f = 0$
Experimental data
Fitting curve
Glass transition region
Phase evolution function ϕ_f
Temperature T(K)
(b)
T_g=330K
T_g=335K
T_g=340K
T_g=345K
332.6K
337.8K
343.3K
349.5K
Phase evolution function ϕ_f
Temperature T(K)

Figure 1.

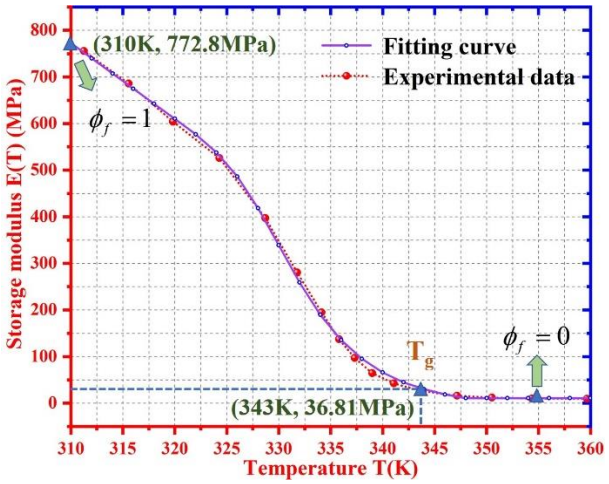
(310K, 772.8MPa)
Fitting curve
Experimental data
$\phi_f = 1$
$\phi_f = 0$
T_g
(343K, 36.81MPa)
Storage modulus E(T) (MPa)
Temperature T(K)
800
700
600
500
400
300
200
100
0
310
315
320
325
330
335
340
345
350
355
360

Figure 2.

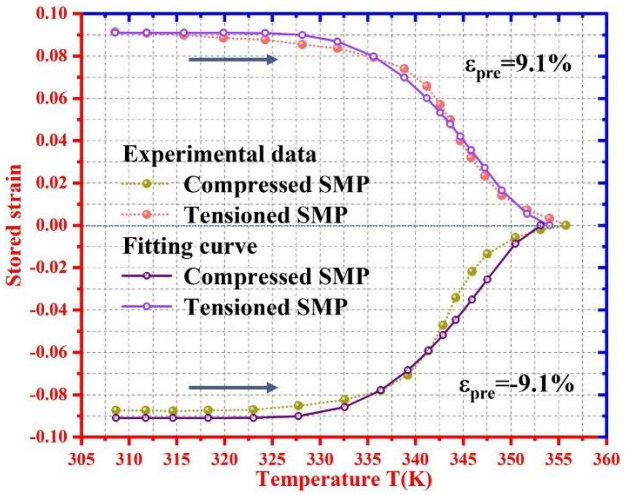
0.10
0.08
0.06
0.04
0.02
0.00
-0.02
-0.04
-0.06
-0.08
-0.10
Stored strain
305
310
315
320
325
330
335
340
345
350
355
360
Temperature T(K)
Experimental data
Compressed SMP
Tensioned SMP
Fitting curve
Compressed SMP
Tensioned SMP
εpre=9.1%
εpre=-9.1%

Figure 3.

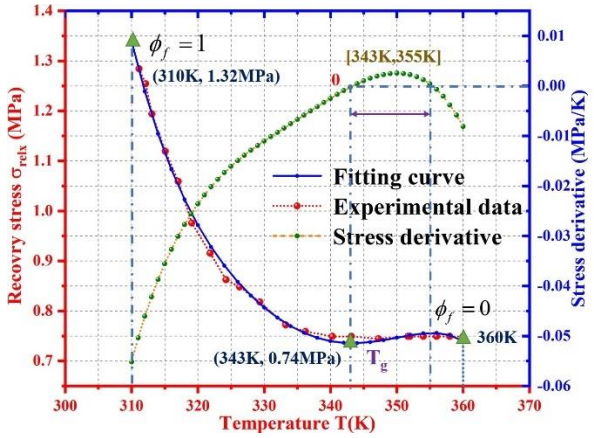
$\phi_f = 1$
(310K, 1.32MPa)
[343K,355K]
0
Fitting curve
Experimental data
Stress derivative
$\phi_f = 0$
360K
(343K, 0.74MPa)
T_g
Recovry stress σ_{relx} (MPa)
Stress derivative (MPa/K)
Temperature T(K)
1.4
1.3
1.2
1.1
1.0
0.9
0.8
0.7
0.01
0.00
-0.01
-0.02
-0.03
-0.04
-0.05
-0.06
300
310
320
330
340
350
360
370

Figure 4.

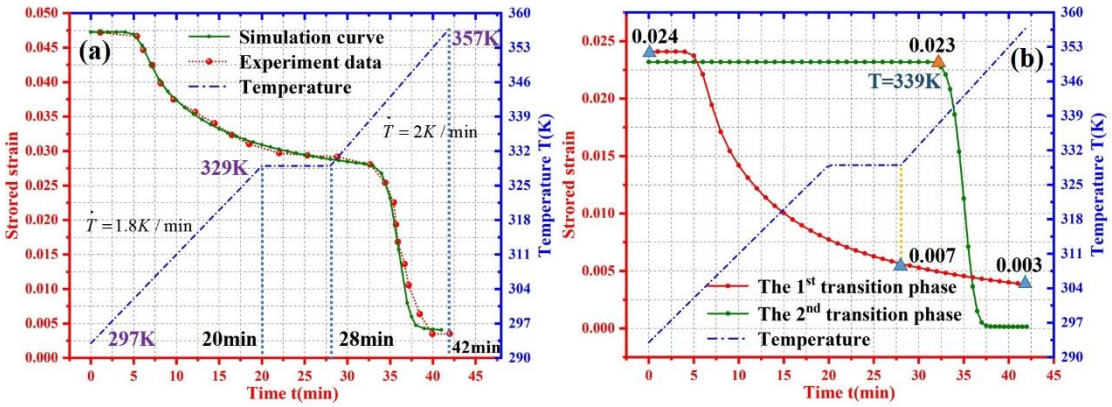
(a)
Simulation curve
Experiment data
Temperature
357K
329K
297K
20min
28min
42min
$\dot{T}=2K/\min$
$\dot{T}=1.8K/\min$
Strored strain
Temperature T(K)
Time t(min)
(b)
0.024
0.023
T=339K
0.007
0.003
The 1st transition phase
The 2nd transition phase
Temperature
Strored strain
Temperature T(K)
Time t(min)

Figure 5.

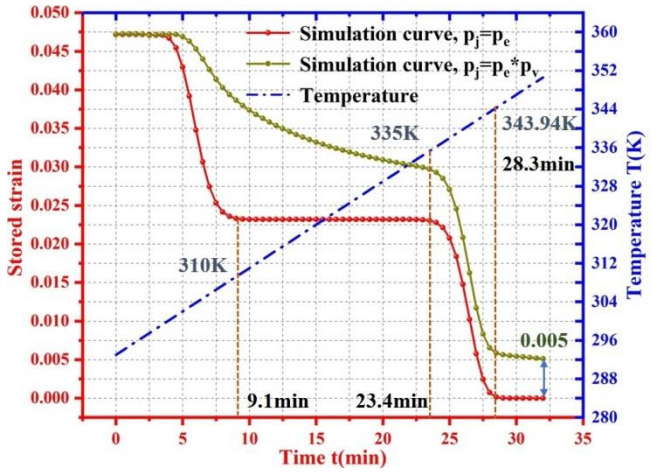
Simulation curve, $p_j=p_e$
Simulation curve, $p_j=p_e*p_v$
Temperature
335K
343.94K
28.3min
310K
0.005
9.1min
23.4min
Stored strain
Temperature T(K)
Time t(min)

Figure 6.

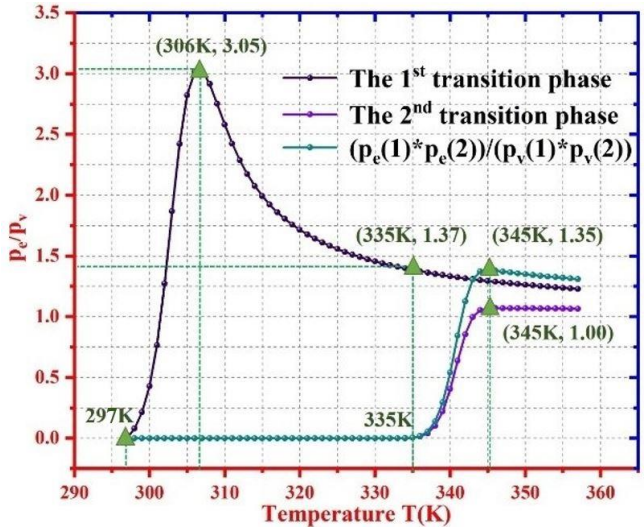
(306K, 3.05)
The 1st transition phase
The 2nd transition phase
(pe(1)*pe(2))/(pv(1)*pv(2))
(335K, 1.37)
(345K, 1.35)
(345K, 1.00)
297K
335K
Pe/Pv
Temperature T(K)
3.5
3.0
2.5
2.0
1.5
1.0
0.5
0.0
290
300
310
320
330
340
350
360

Figure 7.

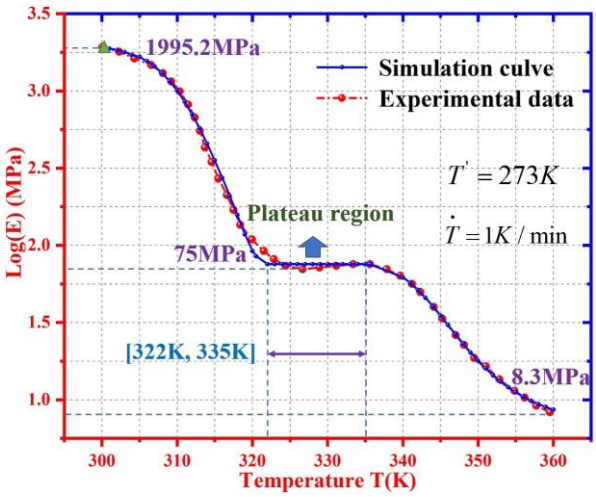
1995.2MPa
Simulation culve
Experimental data
$T^{'} = 273K$
$\dot{T} = 1K / \min$
Plateau region
75MPa
[322K, 335K]
8.3MPa
Log(E) (MPa)
Temperature T(K)
3.5
3.0
2.5
2.0
1.5
1.0
300
310
320
330
340
350
360

Figure 8.

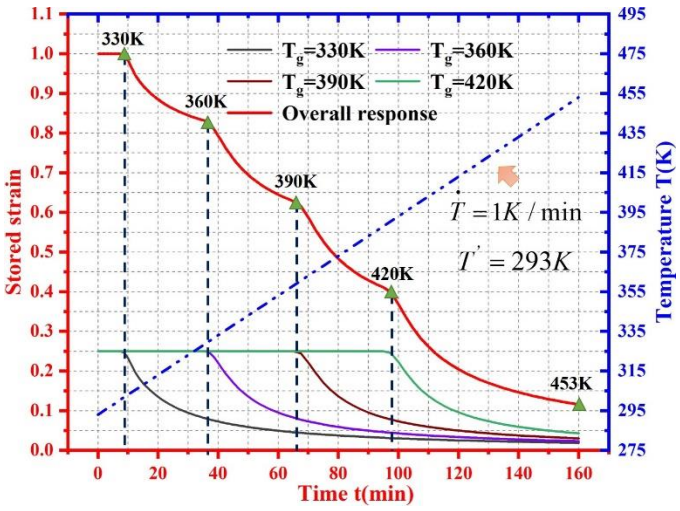
330K
360K
390K
420K
453K
T_g=330K
T_g=360K
T_g=390K
T_g=420K
Overall response
$T = 1K / \min$
$T^{'} = 293K$
Stored strain
Temperature T(K)
Time t(min)
0
20
40
60
80
100
120
140
160
0.0
0.1
0.2
0.3
0.4
0.5
0.6
0.7
0.8
0.9
1.0
1.1
275
295
315
335
355
375
395
415
435
455
475
495

Figure 9.